European Journal of Pharmaceutics and Biopharmaceutics 125 (2018) 28–37

Contents lists available at ScienceDirect

European Journal of Pharmaceutics and Biopharmaceutics

journal homepage: www.elsevier.com/locate/ejpb

Research paper

A hybrid approach to predict the relationship between tablet tensile strength and compaction pressure using analytical powder compression

Ann-Sofie Persson*, Göran Alderborn

Department of Pharmacy, Uppsala University, Box 580, SE-751 23 Uppsala, Sweden

ARTICLE INFO

Keywords:
Prediction
Compression
Compaction
Tablet tensile strength
Yield pressure

ABSTRACT

The objective was to present a hybrid approach to predict the strength-pressure relationship (*SPR*) of tablets using common compression parameters and a single measurement of tablet tensile strength. Experimental *SPR* were derived for six pharmaceutical powders with brittle and ductile properties and compared to predicted *SPR* based on a three-stage approach. The prediction was based on the Kawakita b^{-1} parameter and the in-die Heckel yield stress, an estimate of maximal tensile strength, and a parameter proportionality factor α. Three values of α were used to investigate the influence of the parameter on the *SPR*. The experimental *SPR* could satisfactorily be described by the three stage model, however for sodium bicarbonate the tensile strength plateau could not be observed experimentally. The shape of the predicted *SPR* was to a minor extent influenced by the Kawakita b^{-1} but the width of the linear region was highly influenced by α. An increased α increased the width of the linear region and thus also the maximal predicted tablet tensile strength. Furthermore, the correspondence between experimental and predicted *SPR* was influenced by the α value and satisfactory predictions were in general obtained for $\alpha = 4.1$ indicating the predictive potential of the hybrid approach.

1. Introduction

Analytical powder compression (APC) deals with the assessment of particle mechanical and friction properties from confined powder compression data. Knowledge on particle mechanics and friction properties can subsequently be used to predict powder properties during processing involving mechanical straining, such as milling, blending and compaction. Thus, inherent in the concept of APC is both the assessment and the prediction of properties of particulate materials. Since APC is a tableting process mimicking approach for particle analysis, it may be especially useful in order to couple particle mechanics to compact forming ability, i.e. compactibility [1].

Pharmaceutical tablets are commonly manufactured by confined compression of a powder. The formation of a coherent tablet requires a certain amount of applied force or pressure and the inter-particle bonding generally increases with the applied compaction pressure. The compactibility is from a processing view preferably described by a tablet strength-compaction pressure relationship (*SPR*) since a *SPR* indicates the required compaction pressure during tablet manufacture giving tablets of suitable tensile strength. Generation of a *SPR* is, however, time consuming and typically requires a substantial amount of powder which may be an obstacle at an early stage formulation development. Thus, a simplified procedure for generation of *SPR* for powders is needed but such a procedure has not yet been developed. Based on a multivariate study on the compaction of some model powders, Klevan [2] concluded that a generalised approach to predict the tablet tensile strength from compression parameters was not possible. This problem may however be overcome by using a hybrid approach based on the use of two compression parameters combined with a single indication of tablet tensile strength, i.e. a reference value of tablet tensile strength. The latter involves no further preparation of tablets (and thus no further material consumption) if the tablet is collected from the compression analysis and thereafter characterised with respect to tensile strength. The objective of this paper was to present an approach to derive a predicted *SPR* (SPR_{pred}) and to compare this with an experimental *SPR* (SPR_{exp}), i.e. to evaluate if the SPR_{pred} represents a useful approximation of the SPR_{exp}. A series of SPR_{exp} was obtained by the compaction of six model powders that were selected to represent both plastic and brittle materials.

2. Theory

The strength-pressure relationship of powders has been reported to consist of three regions; a low (first), an intermediate (second), and a high (third) pressure region (Fig. 1) [3]. The low pressure region signifies a pressure region where no tablets are formed, i.e. the pressure is

* Corresponding author.
E-mail address: ann-sofie.persson@farmaci.uu.se (A.-S. Persson).

https://doi.org/10.1016/j.ejpb.2017.12.011
Received 10 October 2017; Received in revised form 18 December 2017; Accepted 20 December 2017
Available online 23 December 2017

Symbols

a	Kawakita parameter (MPa)
b^{-1}	Kawakita parameter (MPa)
P	Pressure (MPa)
P_{c1}	First critical pressure (MPa)
$P_{c1,pred}$	Predicted first critical pressure (MPa)
P_{c2}	Second critical pressure (MPa)
$P_{c2,pred}$	Predicted second critical pressure (MPa)
P_{ref}	Reference pressure (MPa)
SF_c	Solid fraction during loading (–)
SF_d	Solid fraction during unloading (–)
$SF_d(0)$	Tablet solid fraction after unloading, prior to ejection (–)
$SF_{c/d}$	Solid fraction during unloading corrected for elastic recovery (–)
SPR	Strength-pressure relationship
SPR_{exp}	Experimental strength-pressure relationship
SPR_{pred}	Predicted strength-pressure relationship
α	Parameter proportionality factor (–)
α_{in-die}	Experimentally determined parameter proportionality factor (–)
Γ	Plasticity parameter (MPa)
Γ_{pred}	Predicted plasticity parameter (MPa)
ε	Porosity of the powder column (–)
ρ_{app}	Apparent particle density (g/cm^3)
ρ_{bulk}	Poured bulk density (g/cm^3)
σ_t	Tablet tensile strength (MPa)
$\sigma_{t,max}$	Maximal tablet tensile strength (MPa)
$\sigma_{t,max\ pred}$	Maximal predicted tablet tensile strength (MPa)
$\sigma_{t,pred}$	Predicted tablet tensile strength (MPa)
$\sigma_{t,ref}$	Reference tablet tensile strength (MPa)
σ_y	Heckel yield pressure (MPa)
$\sigma_{y,in-die}$	In-die Heckel yield pressure (MPa)
$\sigma_{y,Buckner}$	In-die Heckel yield pressure corrected for elastic recovery (MPa)
$\sigma_{y,out-of-die}$	Out-of-die Heckel yield pressure (MPa)

too low for the particles to cohere into a compact. The intermediate pressure region represents a region where the tablet tensile strength (σ_t) increases with applied compaction pressure, not infrequently in a linear way. Hence, an increased number or area of inter-particle bonds are continuously formed with increased load and it is assumed that the evolution of the inter-particle bond network corresponds to an increase in the inter-particulate contact area over the cross sectional area of the tablet up to a critical point. It is further assumed that the development of contact between particles in the pressure dependent region is controlled by the effective plasticity of the particles. Thereafter, the tablet tensile strength cannot increase further and the high pressure region is reached. The high pressure region denotes a region where no additional alteration of the inter-particle bonding network occurs with increased pressure i.e. the maximal tablet tensile strength ($\sigma_{t,max}$) is reached. The transitions between the first and the second regions, and between the second and the third regions may be described by two critical pressures; the first (lower) critical pressure (P_{c1}) and the second (upper) critical pressure (P_{c2}). Hence, by approximating the experimental SPR (SPR_{exp}) with a three stage model of a tablet strength-pressure relationship, the

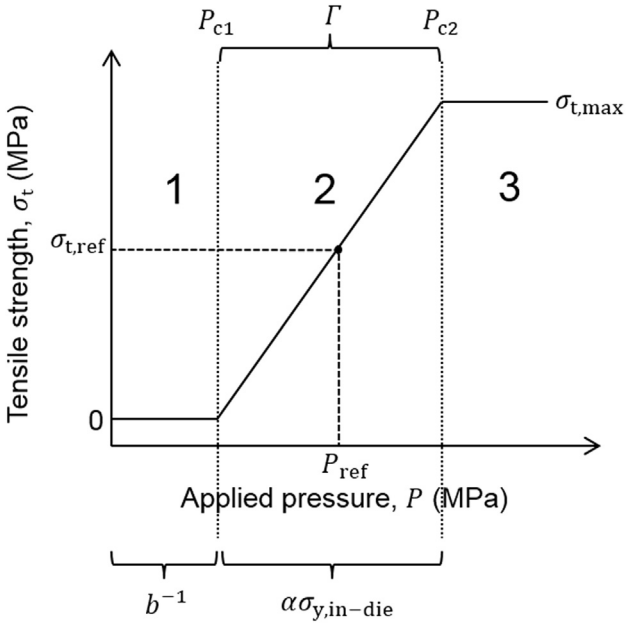

Fig. 1. Schematic illustration of the strength-pressure relationship, its three pressure regions, and the parameters estimates used for prediction.

SPR_{exp} can be described by three compaction parameters P_{c1}, P_{c2}, and Γ. The third parameter Γ corresponds to the width (the difference between the upper and the lower critical pressures, i.e. $P_{c2}-P_{c1}$) of the second region of the SPR_{exp} and can thus be referred to as a plasticity parameter. This second region was assumed to be linear.

In order to calculate a SPR_{pred}, estimates of the three compaction parameters must be derived and in this paper, some common compression parameters obtained from a force-displacement profile obtained by powder compression are used. Firstly, the first critical pressure required for formation of a coherent tablet (P_{c1}) has previously been suggested to be described by the Kawakita b^{-1} parameter [2]. Secondly, the width of the second region (Γ) may be deduced from the assumption that the σ_t of the tablet is controlled by the contact area formed between the particles during compression and that the contact area depends on the particle effective plasticity. The parameter Γ represents thus in principle the effective hardness of the particles and can be calculated by combining the in-die Heckel yield stress ($\sigma_{y,in-die}$), commonly used as an indication of particle plasticity, and a parameter proportionality factor (α). The α is conceptually similar to a constraint factor and can be expected to have a value of about 3 [4]. Such a factor vary between materials and the numerical value of α is in this study *a priori* unknown and is determined empirically. It should be pointed out that the $\sigma_{y,in-die}$ may be influenced by the elastic deformation of the particles during compression depending on their elastic stiffness [5]. More on, the constraint factor between hardness and in-die yield pressure may also be affected by the elastic stiffness of the materials [6] and material dependent constraint factors have previously been reported [7]. Thirdly, the pressure at which the tensile strength plateau is reached (P_{c2}) can be obtained as the sum of P_{c1} and Γ i.e. $\alpha\sigma_{y,in-die} + b^{-1}$ (Fig. 1). The three compaction parameters reflect different powder properties but the parameters are interrelated to each other, i.e. the value of one compaction parameter can be calculated from values of the other two compaction parameters. Henceforth, the predicted compaction parameters will be denoted $P_{c1,pred}$, Γ_{pred}, and $P_{c2,pred}$.

To complete the calculation of the SPR_{pred}, an indication of the maximal tensile strength ($\sigma_{t,max}$) is needed which can be obtained using Eq. (1) and by using the reference value of the tensile strength of the tablets ($\sigma_{t,ref}$) prepared at a reference pressure (P_{ref}) (Fig. 1),

$$\sigma_{t,max\ pred} = \frac{\sigma_{t,ref} * \alpha\sigma_{y,in-die}}{P_{ref} - b^{-1}}. \quad (1)$$

One should note that this procedure of predicting $\sigma_{t,max\ pred}$ is valid when $P_{c2,pred} > P_{ref}$. In a case when $P_{c2,pred} \leq P_{ref}$, $\sigma_{t,ref}$ is to be used as an indication of $\sigma_{t,max\ pred}$. Thus, the choice of procedure used to derive an indication of the maximal tablet tensile strength depends on the ratio

between the effective particle hardness ($\alpha\sigma_{y,in-die}$) and the effective compaction pressure ($P_{ref}-b^{-1}$). The criterion $P_{c2,pred} > P_{ref}$ is valid for a ratio above one and the criterion $P_{c2,pred} \leq P_{ref}$ is valid for a ratio of one and below. Since it is preferable to use a high reference pressure, the former criterion applies to hard materials and the latter to soft materials.

Finally, the SPR_{pred} is constructed by calculating predicted tablet tensile strength values ($\sigma_{t,pred}$) according to Eq. (2) for compaction pressures in the range $P_{c1,pred} \leq P \leq P_{c2,pred}$,

$$\sigma_{t,pred} = \frac{\sigma_{t,max\ pred} * (P-b^{-1})}{\alpha\sigma_{y,in-die}}. \quad (2)$$

An overview of the estimates of the parameters and variables needed is presented in Table 1.

3. Materials

Bulk powders of α-lactose monohydrate (Pharmatose 200M, DMV, The Netherlands), β-lactose (Sigma-Aldrich, Sweden), microcrystalline cellulose (MCC, Avicel PH101, FMC, Ireland), sodium chloride (NaCl, Sigma-Aldrich, Sweden), polyethylene glycol 10 000 (PEG, Alfa Aesar GmbH & Co KG, Karlsruhe, Germany), and sodium bicarbonate (Sigma-Aldrich, Sweden) were used as model materials. The powders were stored in a desiccator for at least 7 days above a saturated solution of magnesium chloride (Sigma-Aldrich, Sweden) generating a relative humidity (RH) of approximately 33% prior to further characterisation. Magnesium stearate (Sigma-Aldrich, Sweden) was used as lubricant. The experiments were made in a humidity controlled room at 30 ± 5% RH and 22 ± 3 °C.

4. Methods

4.1. Scanning electron microscopy

Scanning electron microscopy (SEM) images were captured to enable visualisation of the particle morphology. A single layer of powder was attached to metal stubs using double-adhesive carbon tape. Subsequently, the powders were sputtered (Polaron, Quorum Technologies Ltd., Newhaven, U.K.) with gold/palladium under argon. Images were taken at three magnifications 250×, 500×, and 1000× using the SEM microscope (Leo (Zeiss) 1550 Schottky, Germany) at an accelerating voltage of 2.0 kV.

4.2. Density measurements

Helium displacement pycnometry (AccuPyc 1330, Micromeritics, U.S.) was used to measure the apparent particle density (ρ_{app}, *number of independent measurements,* $n = 3$). Each measurement was an average of ten repeated cycles.

10 ml of powder ($n = 3$) was manually poured through a funnel into a 10 ml glass measuring cylinder (11.1 mm diameter) and weighed to determine the poured bulk density (ρ_{bulk}). The cylinder had a similar diameter as the die cavity used in the compression enabling calculations of powder bed height during powder compression analysis.

4.3. Powder compression analysis

400 mg of powder was uniaxially compressed ($n = 5$) in a materials tester (Zwick Z100, Zwick/Roell GmbH & Co, Ulm, Germany) mounted with a stationary lower and a movable upper punch (11.3 mm diameter). A load of 500 MPa was applied at a rate of 10 mm/min. Prior to die filling, the punches and the die were lubricated with a 1% (w/w) magnesium stearate in ethanol (95%) suspension to reduce frictional forces. The system deformation (0.4 μm/MPa) was measured by pressing the upper and the lower punch together to 500 MPa and this was corrected for in the calculations of powder bed height as described by Nordström et al. [8]. The tablet tensile strength of the tablets formed during compression was subsequently used in the predictions as $\sigma_{t,ref}$ for all materials except for MCC.

Powder compression analysis was made using the Heckel [9] and the Kawakita [10] equations. Firstly, the Heckel equation was used to calculate the in-die yield pressure ($\sigma_{y,\ in-die}$) of the materials using an Excel (Microsoft Corporation) macro for identification of the linear region of the porosity-pressure relationship ($R^2 > 0.999$) as described in detail by Mahmoodi et al. [11]. Briefly, the middle value of the pressure range used in the linear regression analysis was determined from the minimum value of the first derivative. The lowest and the highest pressure values were determined from the 25% increase of the first derivative in both directions. Secondly, the linear form of the Kawakita equation was used to calculate the Kawakita constants a and b^{-1}. a and $1/ab$ were determined by linear regression from the inverse of the slope and the intercept of the linear region, respectively, in the pressure interval 20–495 MPa ($R^2 > 0.999$). b^{-1} was calculated as the product of a and $1/ab$.

In addition, the solid fraction during loading (SF_c) was corrected for elastic recovery during unloading ($SF_{c/d}$) by subtracting the solid fraction during unloading (SF_d) as $SF_{c/d} = SF_c - [SF_d - SF_d(0)]$ and described by Katz et al. [12]. The $SF_d(0)$ denotes the tablet solid fraction when the tablet is fully unloaded but prior to tablet ejection. This was used to derive a Heckel profile corrected for elastic recovery i.e. similar to an out-of-die Heckel profile but consuming less powder material. This corrected Heckel profile is henceforth referred to as the Buckner-Heckel profile and the corresponding σ_y is denoted $\sigma_{y,Buckner}$. The same pressure range was used for calculation of $\sigma_{y,Buckner}$ as used for calculation of $\sigma_{y,in-die}$.

4.4. Tablet compaction

Tablets were compacted in a single-punch press (Korsch EK0, Germany) mounted with 5.65 mm or 11.3 mm diameter flat-faced punches. The distance between the punches was adjusted using a metal stub of 2.0 mm (for 5.65 mm punches) or 3.0 mm (for 11.3 mm punches) height. The punch separation distance was adjusted until a pressure of 5 MPa on the metal stubs was generated. The compaction pressure was hence regulated by the amount of powder in-die. Pressures were applied in a range from 12 to 1000 MPa ($n = 5$ at each pressure). The punches and the die were lubricated prior to compaction as described above (Section 4.3).

The tablet weight, height, and diameter were measured (Litematic VL 50A, Mitutoyo, Japan) and used in combination with the radial tablet fracture force for calculations of tablet tensile strength (σ_t) according to Fell and Newton [13]. The radial tablet fracture force was measured using two types of tablet strength testers; either the PharmaTest (PharmaTest, PTB311E, Hainburg, Germany) or the Holland C50 (U.K.). The PharmaTest was run at a rate of 20 N/s and was in general used for forces up to ~300 N whereas the Holland C50 operated at 1 mm/min and was in general used for forces between ~300 and 500 N. The equipment used appeared to have no impact on the determined σ_t since no deviation occurred in the *SPR* when interchanging strength tester. This instrument setup was additionally used for assessing $\sigma_{t,\ ref}$ of the tablets produced in the materials tester (Section 4.3).

The tablet density was calculated using the tablet weight and the tablet dimensions for calculation of tablet porosity as 1-(tablet density/ρ_{app}). The change in tablet porosity with pressure was analysed using the Heckel equation to derive an out-of-die yield stress ($\sigma_{y,out-of-die}$) in a similar pressure range as in the derivation of $\sigma_{y,in-die}$.

4.5. Strength-pressure analysis

The SPR_{exp} was approximated by a three-stage model [3] and the

Table 1
Overview of the estimates of the parameters and variables during strength-pressure prediction.

Parameter/Variable	Estimate	Criterion
$P_{c1,pred}$	b^{-1}	
Γ_{pred}	$\alpha\sigma_{y,in-die}$	
$P_{c2,pred}$	$b^{-1} + \alpha\sigma_{y,in-die}$	
$\sigma_{t,max\ pred}$	$\frac{\sigma_{t,ref}\,\alpha\sigma_{y,in-die}}{P_{ref} - b^{-1}}$	$P_{c2,pred} > P_{ref}$
$\sigma_{t,max\ pred}$	$\sigma_{t,ref}$	$P_{c2,pred} \leq P_{ref}$
$\sigma_{t,pred}$	$\frac{\sigma_{t,max\ pred}(P - b^{-1})}{\alpha\sigma_{y,in-die}}$	$P_{c1,pred} \leq P \leq P_{c2,pred}$

α: Parameter proportionality factor.
b^{-1}: Kawakita parameter.
Γ_{pred}: Predicted plasticity parameter.
P: Applied pressure.
$P_{c1,pred}$: Predicted first critical pressure.
$P_{c2,pred}$: Predicted second critical pressure.
P_{ref}: Reference pressure.
$\sigma_{t,pred}$: Predicted tablet tensile strength.
$\sigma_{t,max\ pred}$: Predicted maximal tablet tensile strength.
$\sigma_{y,in-die}$: In-die Heckel yield stress.
$\sigma_{t,ref}$: Tablet reference tensile strength.

three compaction parameters describing the three pressure regions, i.e. the lower critical pressure (P_{c1}), the upper critical pressure (P_{c2}), and the compaction parameter (Γ), were determined accordingly. The P_{c1} was determined from extrapolation of the lower linear pressure region (i.e. the 4 lowest pressures) of the SPR_{exp} assessed by linear regression ($R^2 > 0.979$). However, for NaCl the lowest pressure was removed and the subsequent four pressures were used in the regression analysis due to large linear deviation of the first pressure point. The P_{c2} was calculated from the intersection of the regression line of the second region ($R^2 > 0.972$) and the average σ_t of the four highest compaction pressures. The selection of the pressures in the determination of the lower and the upper critical pressures was based on the ambition to obtain the best possible fit of a regression line to the experimental profiles when using a consistent procedure for all six materials. Due to capping problems at large pressures for sodium bicarbonate the tensile strength plateau was difficult to define and thus the P_{c2} was not determined. The Γ was calculated as the reciprocal of the slope obtained by linear regression ($R^2 > 0.987$) of the relative tensile strength $\left(\frac{\sigma_t}{\sigma_{t,max}}\right)$ and the effective applied pressure ($P - P_{c1}$) according to [3]:

$$\frac{\sigma_t}{\sigma_{t,max}} = \frac{1}{\Gamma}\left(P - P_{c1}\right) \quad (3)$$

Eq. (3) corresponds to a definition of Γ as the width of region two, i.e. $P_{c2} - P_{c1}$. The pressure ranges used for the calculations of the compaction parameters are listed in Table 2.

4.6. Strength-pressure prediction

The SPR_{pred} was constructed based on estimates of the compaction parameters and the tensile strengths according to Table 1. The predictions were performed using three values of the parameter proportionality factor α. These were selected as the first quartile (2.5), the median (3.3), and the third quartile (4.1) of the cumulative frequency distribution (Fig. 2) of the experimentally determined α (denoted α_{in-die}); calculated as $\Gamma/\sigma_{y,in-die}$. Moreover, the single indication of tablet tensile strength i.e. $\sigma_{t,ref}$ was selected from the tablet compressed at P_{ref} = 500 MPa for all materials except for MCC. The tablet strength tester was unable to fracture the MCC tablets compressed at 500 MPa, thus for MCC additional tablets were compressed at P_{ref} = 300 MPa using the materials tester as described in Section 4.3.

Table 2
Compaction pressure ranges used in the linear regressions for calculations of the experimental compaction parameters.

Material	Pressure range (MPa)		
	P_{c1}	P_{c2}	Γ
α-lactose	20–48	20–643	20–643
β-lactose	20–73	20–406	20–406
MCC	13–54	13–121	13–121
NaCl	47–98	47–250	47–250
PEG	13–40	13–40	13–40
Sodium bicarbonate	102–201	–	102–598

P_{c1}: First critical pressure.
P_{c2}: Second critical pressure.
Γ: Plasticity parameter.

5. Results and discussion

5.1. Particle characteristics

The scanning electron microscopy (SEM) images (Fig. 3) showed that powders of α-lactose, NaCl, PEG, and sodium bicarbonate consisted of primary particles whereas in powders of β-lactose and MCC, secondary particles, i.e. agglomerates, occurred. The presence of particle agglomerates may affect the compaction and compression behaviour of the powder compared to powders consisting of primary particles. It is for example reported [14] that a correct derivation of yield pressure using the Heckel relationship is difficult for agglomerates. The SEM images indicated also a large spread in particle size distribution for all powders. This is not unexpected as the powders were used as supplied from the manufacturer without any further size separation.

The apparent particle density (ρ_{app}) and the poured bulk density (ρ_{bulk}) of the powders are listed in Table 3.

5.2. Compression characteristics

The inverse of the slope of the linear region of the Heckel relationship is often used as an indication of the yield pressure of particles (σ_y), i.e. particle effective plasticity [9]. Powders of PEG [15], MCC, and NaCl are often reported to deform during compression [7] whereas both α- and β-lactose are reported to fragment to a large degree during compression [7]. Moreover, sodium bicarbonate is reported to have a high σ_y i.e. have a high plastic stiffness [16]. However, sodium bicarbonate is in addition reported to show limited fragmentation during compression [16,17]. Thus, sodium bicarbonate can be classified as a plastic but hard material. Thus, the selected materials comprise a broad

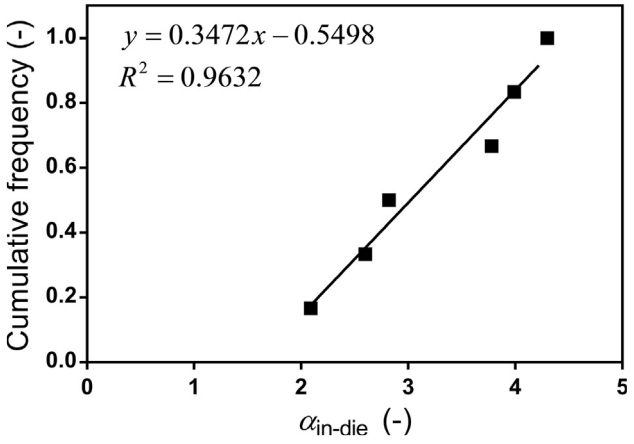

Fig. 2. Cumulative frequency of α_{in-die}.

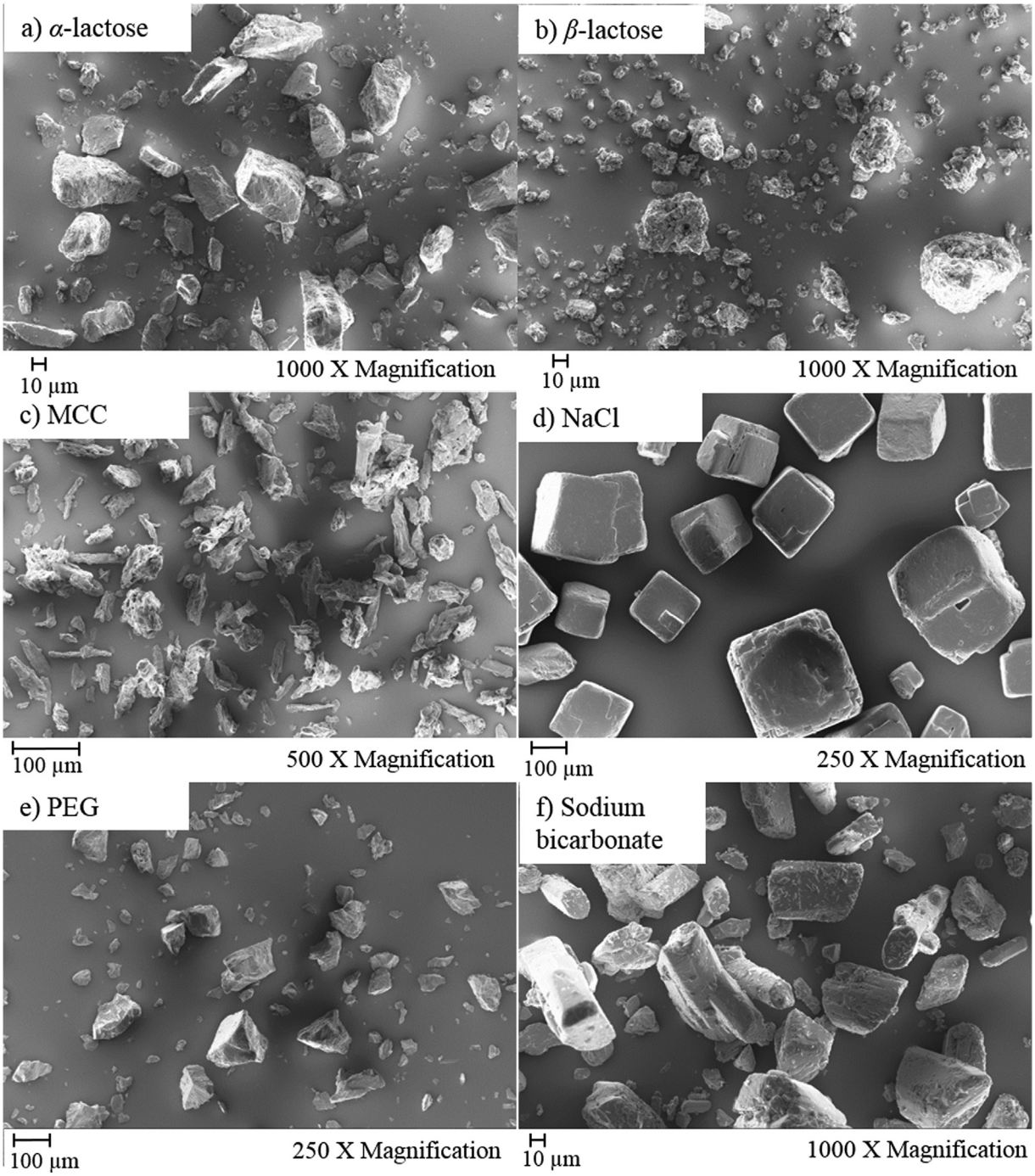

Fig. 3. Scanning electron microscopy images of studied powder materials. Note the varying image magnifications and thus the varying scale bars.

Table 3
Density characteristics. Relative standard deviations (n = 3) are given in parentheses.

Material	ρ_{app} (g/cm^3)	ρ_{bulk} (g/cm^3)
α-lactose	1.537 (0.00)	0.52 (0.01)
β-lactose	1.574 (0.00)	0.64 (0.01)
MCC	1.582 (0.00)	0.32 (0.04)
NaCl	2.154 (0.00)	1.3 (0.01)
PEG	1.229 (0.00)	0.59 (0.02)
Sodium bicarbonate	2.217 (0.00)	0.97 (0.01)

ρ_{app}: Apparent particle density.
ρ_{bulk}: Poured bulk density.

range of mechanical characteristics which indeed were reflected in the in-die Heckel profiles (Fig. 4) and thus the corresponding in-die yield pressures ($\sigma_{y,in-die}$). The $\sigma_{y,in-die}$ (Table 4) ranged from 22.0 MPa for PEG to 295 MPa for sodium bicarbonate and thus the materials can be classified as being very soft (PEG), soft (NaCl), moderately hard (MCC, α-lactose, and β-lactose) and hard (sodium bicarbonate) according to Roberts and Rowe [7].

The shape of the Heckel profiles was as expected highly dependent on whether the porosity (ε) data was collected in-die or out-of-die (compare solid line and dots in Fig. 4). The in-die Heckel profiles displayed a more rapid decrease in ε compared to the out-of-die Heckel profiles, which is due to the elastic contribution during in-die compression, as also indicated by the linear deviation at high compression

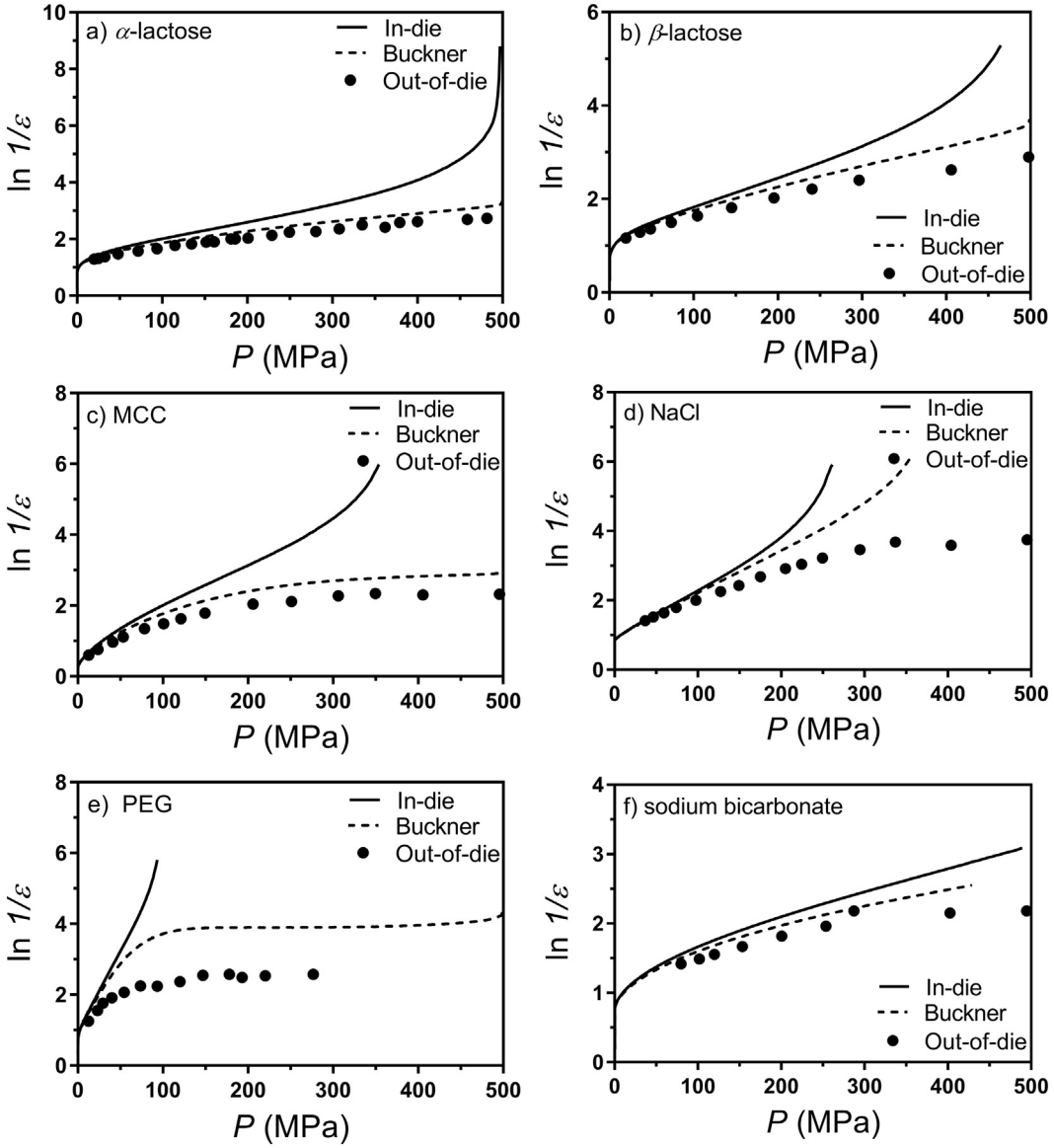

Fig. 4. Heckel profiles derived using in-die data (solid lines), out-of-die data (dots), and in-die data corrected for elastic recovery according to Buckner (dashed lines). Note the varying scale of the y-axes.

pressures. Hence, the corresponding out-of-die yield pressure ($\sigma_{y,out-of-die}$) is considerably higher than $\sigma_{y,in-die}$ (Table 4). The $\sigma_{y,out-of-die}$ may be the preferred indication of the plasticity of the particles as the elastic contribution is smaller. Hence, the $\sigma_{y,out-of-die}$ would theoretically be a better parameter in the calculation of the plasticity parameter (Γ). However, the generation of an out-of-die Heckel profile is both time and material consuming. An alternative is to generate an out-of-die Heckel profile based on in-die data according to Buckner and coworkers [12]. For the materials investigated in this paper, the Buckner-Heckel profiles were intermediate between the in-die and the out-of-die Heckel profiles. For α-lactose, β-lactose, MCC, and sodium bicarbonate, the Buckner-Heckel profiles showed a better agreement to the out-of-die profiles than the in-die profiles (Fig. 4) while for NaCl and PEG, two materials known for their plastic properties [7,15], the reverse applied. The $\sigma_{y,out-of-die}$ values were between a factor 1.2–1.4 larger than the Buckner yield stress ($\sigma_{y,Buckner}$) values for all materials except for sodium bicarbonate for which the ratio was larger (2.3) (Table 4). Comparing the yield pressures derived using the in-die and the Buckner approaches it is clear that the spread in σ_y using both approaches was similar. Since the Buckner approach requires additional data handling and since there is a need to define the parameter proportionality factor (α) irrespective of which type of σ_y that is to be used, the more common indication of particle plasticity, i.e. $\sigma_{y,in-die}$, was used in the calculation of Γ.

The Kawakita a and b^{-1} parameters are additionally presented in Table 4. The a parameter ranged between 0.45 for NaCl and 0.81 for MCC and the b^{-1} parameter ranged between 4.81 MPa for PEG and 40.4 MPa for NaCl. Thus, these parameters supports further the broad range of compression behaviour of the powders selected for the study.

5.3. Experimental strength-pressure relationships

In, Fig. 5, all experimentally derived strength-pressure relationships (SPR_{exp}) are presented. For all materials, the shape of the SPR_{exp} at low compaction pressures, i.e. close to the first critical pressure (P_{c1}), was slightly sigmoidal. However, the curvature of the initial part of the SPR_{exp} was small and was considered to have a limited influence on the P_{c1}. Hence, the linear regression used for determination of P_{c1} appears to be a justified approximation. The experimentally determined P_{c1} for the studied materials is listed in Table 5.

A satisfactory correspondence between the Kawakita b^{-1} parameter (Table 4) and P_{c1} was obtained for all materials, e.g. for PEG

Table 4
Experimentally measured compression characteristics. Relative standard deviations are given in parentheses (n = 5).

Material	$\sigma_{y,\ in\text{-}die}$ (MPa)	$\sigma_{y,\ out\text{-}of\text{-}die}$ (MPa)	$\sigma_{y,\ Buckner}$ (MPa)	a (–)	b^{-1} (MPa)
α-lactose	168 (0.02)	294	244 (0.03)	0.67 (0.00)	7.21 (0.03)
β-lactose	156 (0.01)	237	195 (0.01)	0.61 (0.00)	13.7 (0.00)
MCC	87.5 (0.02)	221	164 (0.01)	0.81 (0.00)	5.48 (0.01)
NaCl	73.2 (0.00)	111	78.7 (0.01)	0.45 (0.00)	40.4 (0.02)
PEG	22.0 (0.01)	41.1	30.1 (0.01)	0.55 (0.00)	4.81 (0.02)
Sodium bicarbonate	295 (0.02)	941	408 (0.01)	0.55 (0.00)	17.1 (0.01)

$\sigma_{y,\ in\text{-}die}$: Heckel yield stress derived using in-die data.
$\sigma_{y,\ out\text{-}of\text{-}die}$: Heckel yield stress derived using out-of-die data.
$\sigma_{y,\ Buckner}$: Heckel yield stress derived using in-die data corrected for elastic recovery according to Buckner and coworkers [12].
a: Kawakita parameter.
b^{-1}: Kawakita parameter.

b^{-1} = 4.81 MPa vs. P_{c1} = 4.6 MPa, except for sodium bicarbonate for which a substantial difference was obtained (b^{-1} = 17.1 MPa vs. P_{c1} = 44 MPa). It is however concluded that generally b^{-1} approximated P_{c1} in a satisfactory way.

For all powders, the tablet tensile strength (σ_t) increased approximately linearly with increased pressure in the beginning of the second region of the SPR_{exp}. Subsequently with increasing pressures the SPR_{exp} levelled off and reached the σ_t plateau. This transition occurred either gradually, as for β-lactose, MCC, and PEG, or distinct as for α-lactose and NaCl. The σ_t plateau was clearly visible for α-lactose, β-lactose, MCC, NaCl, and PEG (Fig. 5a–e) whereas it was not detectable for sodium bicarbonate (Fig. 5f). For sodium bicarbonate, a plateau seemed to be initiated at pressures ≥ 800 MPa where the SPR_{exp} started to deviate from linearity. At higher pressures the incidence of capping became frequent and a $\sigma_{t,max}$ could thus not be determined.

The SPR_{exp} varied considerably between the materials with both low and high values of P_{c2} and $\sigma_{t,max}$, the latter ranging from below 2 MPa to above 10 MPa (Table 5 and Fig. 5) signifying the large variation in compactibility between the powders. Thus, the selected powders represented a large variation not only in compression behaviour but also in compactibility. The large variation in P_{c2} corresponded to a broad range of Γ values, supporting that the powders showed a large variation in effective plasticity (Table 5). The Γ was lowest for the very soft material PEG, corresponding to that a relatively low load was needed to reach $\sigma_{t,max}$, while the highest Γ was obtained for sodium bicarbonate.

The ratio between the experimentally determined parameters Γ and $\sigma_{y,in-die}$ is referred to as the parameter proportionality factor (α_{in-die}). The α_{in-die} ranged from 2.09 for MCC to 4.30 for α-lactose (Table 5). Despite the various mechanical characteristics and the large variation in Γ values of the studied materials, the α_{in-die} values showed a limited absolute variation. Furthermore, the values of α_{in-die} were close to a value of 3 which is considered a typical value of a particle constraint factor [18].

It is concluded that for all test powders except sodium bicarbonate, the SPR_{exp} could be satisfactorily approximated with the three-stage model [3] (Fig. 5), i.e. coherent tablets were firstly formed at a powder specific pressure threshold (P_{c1}) which was followed by a σ_t increase that could be approximated by a linear relationship and finally, a σ_t plateau was reached.

5.4. Predicted strength-pressure relationships

In order to use in practice the hybrid prediction approach a standardised value of the parameter proportionality factor α is necessary. Using the cumulative distribution of α_{in-die} (Fig. 2) three values were selected to be used in the predictions in order to investigate their influence on the correspondence between SPR_{pred} and SPR_{exp}. The selected values were 2.5 ($\alpha_{2.5}$), 3.3 ($\alpha_{3.3}$), and 4.1 ($\alpha_{4.1}$) as these approximately represented the first quartile, the median, and the third quartile of the cumulative distribution of the α_{in-die}. Thus, three different SPR_{pred} were derived and presented in Fig. 6 together with the SPR_{exp}.

The SPR_{pred} were influenced by the value of α and the criterion for estimating the maximal predicted tablet tensile strength ($\sigma_{t,max\ pred}$) (Table 1). An increased α increased the width of the second region of the SPR and the transition from region two to region three thus occurred at a gradually higher $P_{c2,pred}$. In addition, the $\sigma_{t,max\ pred}$ increased with an increase in α in predictions were the criterion $P_{c2,pred} > P_{ref}$ was valid. For the circumstance where $P_{c2,pred} \leq P_{ref}$, the $\sigma_{t,max\ pred}$ was unaffected by α as the measured reference tensile strength ($\sigma_{t,ref}$) was used as the $\sigma_{t,max\ pred}$.

Regarding the predicted first critical pressure ($P_{c1,pred}$) it was concluded (Section 5.3) that the Kawakita b^{-1} parameter gave a reasonable estimate of the experimental P_{c1} for all materials except for sodium bicarbonate, as evident also in Fig. 6. However, as the value of this parameter was generally low its influence on the overall SPR_{pred} was of minor importance.

For the second region of the SPR, the SPR_{pred} derived using $\alpha_{3.3}$ and $\alpha_{4.1}$ gave better predictions of region two compared to SPR_{pred} derived using $\alpha_{2.5}$ for all materials except for MCC and sodium bicarbonate (Fig. 6). For MCC the prediction of region two was improved using $\alpha_{2.5}$ (green curve in Fig. 6c) whereas for sodium bicarbonate the correspondence was satisfactory for all values of α (Fig. 6f).

The profiles obtained by the prediction procedure demonstrates the influence of α on the estimated parameter values when $P_{c2,pred} > P_{ref}$. For α-lactose, β-lactose, and NaCl, a satisfactory correspondence between $P_{c2,pred}$ and experimental P_{c2} as well as between $\sigma_{t,max\ pred}$ and experimental $\sigma_{t,max}$ were obtained when using $\alpha_{4.1}$ (Tables 5 and 6) with relative deviations between the experimental and the predicted values smaller than 11%. However, the $P_{c2,pred}$ and the $\sigma_{t,max\ pred}$ was somewhat lower for α-lactose and somewhat higher for β-lactose and NaCl than the experimental P_{c2} and $\sigma_{t,max}$. For MCC, $\alpha_{2.5}$ gave the best prediction of $P_{c2,pred}$ although the deviation to the experimental P_{c2} was relatively high while for $\sigma_{t,max\ pred}$ both $\alpha_{2.5}$ and $\alpha_{3.3}$ gave reasonable agreement to experimental data. For PEG, the $P_{c2,pred}$ was satisfactorily predicted using $\alpha_{2.5}$ while the $\sigma_{t,max\ pred}$ deviated markedly from experimental data for all values of α. For sodium bicarbonate finally, a comparison could not be made as the tensile strength plateau could not be experimentally determined.

It is obvious that the best agreement between predicted and experimental values of the parameters $P_{c2,pred}$ and $\sigma_{t,max\ pred}$ is obtained when the α value used is close to the experimentally derived α_{in-die}. However, in order for this hybrid approach to be applicable to routine investigations of powders a standardised value of α is necessary. Considering the agreement between SPR_{pred} and SPR_{exp} reported in Fig. 6, it is concluded that the use of $\alpha_{4.1}$ gave the best overall predictions with regard to both the width and the slope of the second region of the SPR. However, especially for MCC, the SPR_{pred} deviated from SPR_{exp} (Fig. 6c). The deviation may be explained by the presence of agglomerates in the MCC powder (Fig. 3c) making the determination of yield

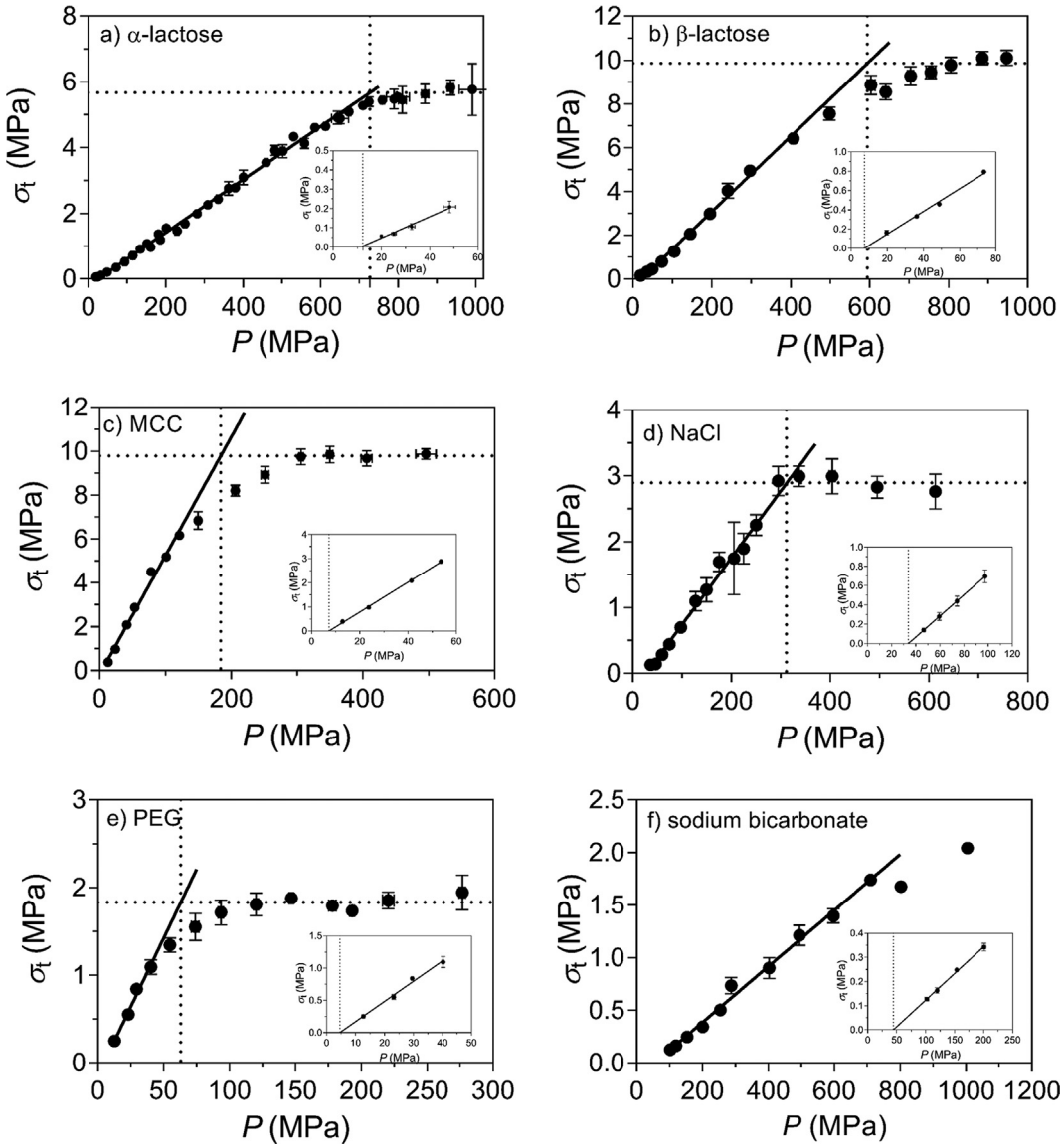

Fig. 5. Experimental strength-pressure relationships (SPR_{exp}). The insets display the initial part of the SPR_{exp} from which the lower critical pressure (P_{c1}) was determined (indicated by the dotted line). In the master plots; the intersection between the linear regressions in the SPR_{exp} and the dashed horizontal lines was used for determination of the upper critical pressure (P_{c2}) (indicated by the dotted vertical line). The error bars denote the standard deviation (n = 5).

Table 5
Experimental compaction characteristics.

Material	P_{c1} (MPa)	P_{c2} (MPa)	Γ (MPa)	$\sigma_{t,max}$ (MPa)	α_{in-die} (–)
α-lactose	11	727	722	5.83	4.30
β-lactose	7.4	594	590	10.1	3.78
MCC	7.3	184	183	9.87	2.09
NaCl	34	311	292	3.00	3.99
PEG	4.6	63.0	62.1	1.94	2.82
Sodium bicarbonate	44	–	769	2.04[a]	2.60

P_{c1}: First critical pressure.
P_{c2}: Second critical pressure.
Γ: Plasticity parameter calculated according to Eq. (3).
$\sigma_{t,max}$: Maximal measured tablet tensile strength.
α_{in-die}: Parameter proportionality factor calculated as $\Gamma/\sigma_{y,in-die}$.
[a] Should not be equalized as the tensile strength plateau.

pressure by powder compression questionable [14]. However, the prediction was satisfactory for the β-lactose powder despite the presence of agglomerates in this powder. Thus, the deviation for MCC may alternatively be explained by the untypical binding capacity of the powder [19]. In terms of the character of the *SPR*, the MCC profile was characterised by an initial steep gradient in region two, a marked bending in the second part of region two and a very high plateau level, i.e. $\sigma_{t,max}$. This type of compaction behaviour may be comparatively difficult to predict in the approach presented here. Nevertheless, the overall *SPR* is captured reasonably by the prediction using the standard value $\alpha_{4.1}$. More on, it is reported that a preferred target value of tablet tensile strength in pharmaceutical manufacturing is within the range of 1–2 MPa [20,21]. One may note that in the relevant range of compaction pressures, i.e. the range giving a preferred target tensile strength, the agreement between experimental and predicted *SPR* was high also for MCC.

One should note that the experimentally determined tablet tensile strength values tended to differ between tablets formed in the materials tester and in the eccentric tablet press at the same compaction pressure. The largest differences in σ_t between tablets compressed with the materials tester and with the tablet press were obtained for PEG (~30%), NaCl (~15%), and sodium bicarbonate (~11%) whereas for α-lactose, β-lactose, and MCC the differences between the σ_t values were smaller

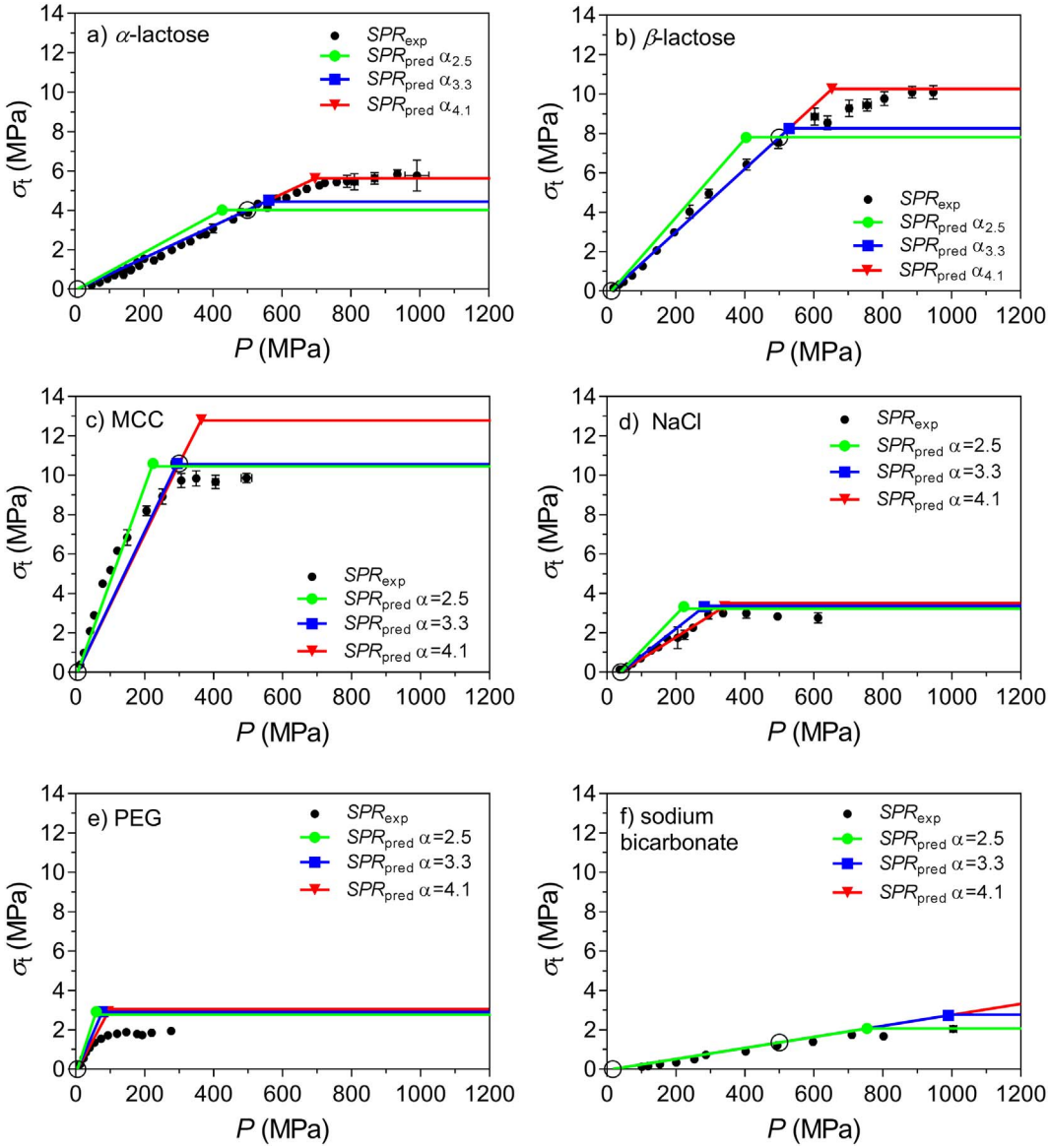

Fig. 6. Comparison between experimental (SPR_{exp}) and predicted strength-pressure relationships (SPR_{pred}) for three values of α. The error bars denote the standard deviations. The open circles at low P represent the predicted first critical pressures ($P_{c1,pred}$) and at P = 500 MPa the reference tensile strength value ($\sigma_{t,ref}$) when $P_{c2,pred} > P_{ref}$.

(< 10%). An important factor behind this material dependent effect of compaction machine is the rate of compression which typically affects the viscous particle deformation in-die [22], and thus the evolution of inter-particulate bonds, and affects the derived value of the yield pressure [4]. It has also earlier been reported that a *SPR* may be affected by the compaction rate [23] and that the strain-rate sensitivity varies between materials [24]. For PEG [25], NaCl, and sodium bicarbonate, the machine dependent differences in σ_t between tablets compressed with the materials tester and with the tablet press is thus explained by a high strain-rate sensitivity. MCC has been reported as being strain-rate sensitive and being strain-rate insensitive [23,26] but it appeared in this study to be strain-rate insensitive. Lactose has previously been reported as strain-rate insensitive [26] which is consistent with the behaviour of both α-lactose and β-lactose in this study. It can thus be concluded that the compression conditions in terms of loading rate may affect an experimental strength-pressure profile but to different extent dependent on the properties of the material. A predicted strength-pressure profile for a given material may thus give better or worse agreement to experimental strength-pressure profiles obtained from different tablet presses operating under different conditions. A key aspect for the possibility to transfer profiles from one tablet press to another is the consistency of the parameter proportionality factor between presses. The parameter proportionality factor is a means to correlate yield stress with tablet strength for a certain experimental setting and another value of the parameter proportionality factor may

Table 6
Predicted upper critical pressures ($P_{c2,pred}$) and predicted maximal tablet tensile strengths ($\sigma_{t,max\ pred}$) for three values of α.

Material	$\alpha_{2.5}$		$\alpha_{3.3}$		$\alpha_{4.1}$	
	$P_{c2,pred}$ (MPa)	$\sigma_{t,max\ pred}$ (MPa)	$P_{c2,pred}$ (MPa)	$\sigma_{t,max\ pred}$ (MPa)	$P_{c2,pred}$ (MPa)	$\sigma_{t,max\ pred}$ (MPa)
α-lactose	427	4.02[a]	562	4.52	696	5.62
β-lactose	404	7.80[a]	529	8.26	653	10.3
MCC	224	10.6[a]	294	10.6[a]	364	12.8
NaCl	223	3.33[a]	282	3.33[a]	341	3.33[a]
PEG	59.8	2.92[a]	77.4	2.92[a]	95.0	2.92[a]
Sodium bicarbonate	755	2.07	991	2.73	1227	3.40

[a] equal to $\sigma_{t,ref}$.

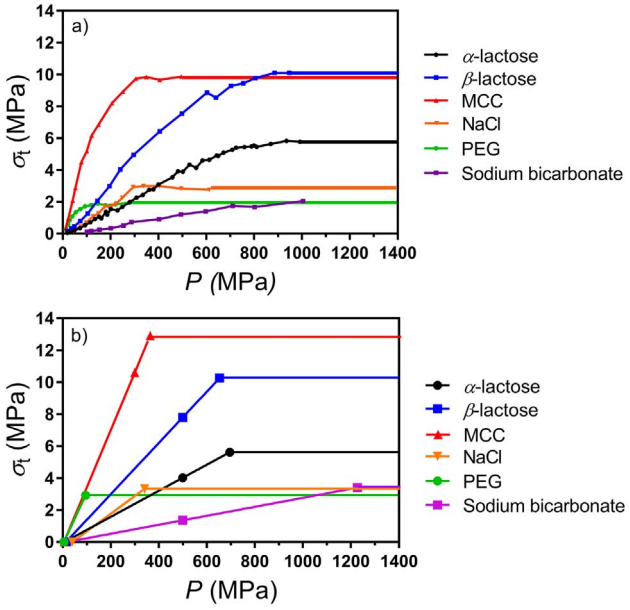

Fig. 7. Overview of experimental (a) and predicted (b) strength-pressure relationships for the studied materials. The predictions were made using $\alpha_{4.1}$.

be needed if other compression conditions are used. However, the issue of transferability to different tablet presses and the role of the parameter proportionality factor deserves to be further investigated by systematic comparisons of different presses.

The hybrid approach for predicting strength-pressure relationships for tablets presented in this paper is based on a simplified description of an SPR_{exp} as consisting of three regions. Two of the test powders, i.e α-lactose and NaCl, displayed distinct transitions between the three regions whereas the transitions were more diffuse for β-lactose, MCC, PEG, and sodium bicarbonate. Nevertheless, the SPR_{exp} for a series of materials with a broad range of physical properties were reasonably captured in the predictions (Fig. 6). In Fig. 7, all SPR_{exp} (Fig. 7a) and SPR_{pred} (Fig. 7b) are presented illustrating that the hybrid approach is able to describe the broad range of compaction behaviour represented by the powders used in this study. It is thus concluded that the hybrid approach gives a satisfactory approximation of SPR_{exp} and a standardised value of the parameter proportionality factor α appears to be practically useful.

6. Conclusions

In this paper, a hybrid approach to predict a tablet strength-compression pressure profile has been presented and evaluated for a series of powders with both ductile and brittle characteristics. The predictions were based on compression parameters in combination with a single indication of tablet tensile strength and a parameter proportionality factor. In general, satisfactory predictions of the experimental strength-pressure relationship were obtained even with a standardised value of the parameter proportionality factor. Highly overlapping experimental and predicted strength-pressure relationships were obtained for two (α-lactose and NaCl) of the studied materials, both showing distinct transitions between the regions of the experimental strength-pressure relationships. For the other four materials, larger deviations between experimental and predicted strength-pressure relationships were obtained due to more diffuse transitions between the regions of the experimental strength-pressure relationships. The approach requires a limited number of experiments and appears thus to be a material sparing yet valuable way of predicting strength-pressure relationships for a powder with the potential to be implemented into early stage tablet formulation development. In order to implement this procedure, a standardised value of the parameter proportionality factor needs to be determined for the experimental setting to be used.

Acknowledgements

Niklas Bunta Sundin is gratefully acknowledged for conducting the compression and the compaction experiments of α-lactose monohydrate. The authors thank Dr. Lucia Lazorova, Department of Pharmacy, Uppsala University for capturing the scanning electron microscopy images.

References

[1] H. Leuenberger, The compressibility and compactibility of powder systems, Int. J. Pharm. 12 (1982) 41–55.
[2] I. Klevan, Compression analysis of pharmaceutical powders: Assessment of mechanical properties and tablet manufacturability prediction, Doctoral Thesis, Comprehensive Summary University of Tromsø, 2011.
[3] G. Alderborn, A novel approach to derive a compression parameter indicating effective particle deformability, Pharm. Dev. Technol. 8 (2003) 367–377.
[4] R.C. Rowe, R.J. Roberts, Mechanical properties, in: G. Alderborn, C. Nyström (Eds.), Pharmaceutical Powder Compaction Technology, Marcel Deeker, New York, 1996, pp. 283–322.
[5] A. Hassanpour, M. Ghadiri, Distinct element analysis and experimental evaluation of the Heckel analysis of bulk powder compression, Powder Technol. 141 (2004) 251–261.
[6] D.M. Marsh, Plastic flow in glass, Proc. R. Soc. London, Ser. A 279 (1964) 420–435.
[7] R.J. Roberts, R.C. Rowe, The compaction of pharmaceutical and other model materials – a pragmatic approach, Chem. Eng. Sci. 42 (1987) 903–911.
[8] J. Nordström, K. Welch, G. Frenning, G. Alderborn, On the physical interpretation of the Kawakita and Adams parameters derived from confined compression of granular solids, Powder Technol. 182 (2008) 424–435.
[9] R.W. Heckel, Density-pressure relationships in powder compaction, T. Metall. Soc. AIME 221 (1961) 671–675.
[10] K. Kawakita, K.-H. Lüdde, Some considerations on powder compression equations, Powder Technol. 4 (1971) 61–68.
[11] F. Mahmoodi, I. Klevan, J. Nordström, G. Alderborn, G. Frenning, A comparison between two powder compaction parameters of plasticity: the effective medium A parameter and the Heckel 1/K parameter, Int. J. Pharm. 453 (2013) 295–299.
[12] J.M. Katz, R. Roopwani, I.S. Buckner, A material-sparing method for assessment of powder deformation characteristics using data collected during a single compression-decompression cycle, J. Pharm. Sci. 102 (2013) 3687–3693.
[13] J.T. Fell, J.M. Newton, Determination of tablet tensile strength by the diametral-compression test, J. Pharm. Sci. 59 (1970) 688–691.
[14] A.S. Persson, J. Nordström, G. Frenning, G. Alderborn, Compression analysis for assessment of pellet plasticity: identification of reactant pores and comparison between Heckel, Kawakita, and Adams equations, Chem. Eng. Res. Des. 110 (2016) 183–191.
[15] H. Larhrib, J.I. Wells, M.H. Rubinstein, Compressing polyethylene glycols: the effect of compression pressure and speed, Int. J. Pharm. 147 (1997) 199–205.
[16] M. Eriksson, G. Alderborn, The effect of particle fragmentation and deformation on the interparticulate bond formation process during powder compaction, Pharm. Res. 12 (1995) 1031–1039.
[17] M. Duberg, C. Nyström, Studies on direct compression of tablets XVII Porosity-pressure curves for the characterization of volume reduction mechanisms in powder compression, Powder Technol. 46 (1986) 67–75.
[18] D. Tabor, Indentation hardness and its measurements: some cautionary comments, in: P.J. Blau, B.R. Lawn (Eds.), Microindentation techniques in materials science and engineering, ASTM Special Technical Publication 889, American society for testing and materials, Philadelphia, 1986, pp. 129–159.
[19] G. Thoorens, F. Krier, B. Leclercq, B. Carlin, B. Evrard, Microcrystalline cellulose, a direct compression binder in a quality by design environment—a review, Int. J. Pharm. 473 (2014) 64–72.
[20] C.Q.C. Sun, H. Hou, P. Gao, C. Ma, C. Medina, F.J. Alvarez, Development of a high drug load tablet formulation based on assessment of powder manufacturability: moving towards quality by design, J. Pharm. Sci. 98 (2009) 239–247.
[21] M. Leane, K. Pitt, G. Reynolds, A proposal for a drug product Manufacturing Classification System (MCS) for oral solid dosage forms, Pharm. Dev. Technol. 20 (2015) 12–21.
[22] K.V. Maarschalk, H. Vromans, G.K. Bolhuis, C.F. Lerk, The effect of viscoelasticity and tabletting speed on consolidation and relaxation of a viscoelastic material, Eur. J. Pharm. Biopharm. 42 (1996) 49–55.
[23] C.K. Tye, C.C. Sun, G.E. Amidon, Evaluation of the effects of tableting speed on the relationships between compaction pressure, tablet tensile strength, and tablet solid fraction, J. Pharm. Sci. 94 (2005) 465–472.
[24] R.J. Roberts, R.C. Rowe, The effect of punch velocity on the compaction of a variety of materials, J. Pharm. Pharmacol. 37 (1985) 377–384.
[25] H. Larhrib, J.I. Wells, Compression of thermally treated Polyethylene glycol 10000, Int. J. Pharm. 153 (1997) 51–58.
[26] R. Ishino, H. Yoshino, Y. Hirakawa, K. Noda, Influence of tabletting speed on compactibility and compressibility of two direct compressible powders under high-speed compression, Chem. Pharm. Bull. 38 (1990) 1987–1992.